Published in final edited form as:
J Phys Chem B. 2013 April 25; 117(16): 4521–4527. doi:10.1021/jp308628y.

Aminoacyl-tRNA Substrate and Enzyme Backbone Atoms Contribute to Translational Quality Control by YbaK

Sandeep Kumar[†,§,⊥], **Mom Das**[†,‡,§], **Christopher M. Hadad**[†], and **Karin Musier-Forsyth**[*,†,‡,§]

[†]Department of Chemistry and Biochemistry, Ohio State University, Columbus, Ohio 43210

[‡]Ohio State Biochemistry Program, Ohio State University, Columbus, Ohio 43210

[§]Center for RNA Biology, Ohio State University, Columbus, Ohio 43210

Abstract

Amino acids are covalently attached to their corresponding tRNAs by aminoacyl-tRNA synthetases. Proofreading mechanisms exist to ensure that high fidelity is maintained in this key step in protein synthesis. Prolyl-tRNA synthetase (ProRS) can misacylate cognate $tRNA^{Pro}$ with Ala and Cys. The *cis*-editing domain of ProRS (INS) hydrolyzes Ala-$tRNA^{Pro}$, whereas Cys-$tRNA^{Pro}$ is hydrolyzed by a single domain editing protein, YbaK, *in trans*. Previous studies have proposed a model of substrate-binding by bacterial YbaK and elucidated a substrate-assisted mechanism of catalysis. However, the microscopic steps in this mechanism have not been investigated. In this work, we carried out biochemical experiments together with a detailed hybrid quantum mechanics/molecular mechanics study to investigate the mechanism of catalysis by *Escherichia coli* YbaK. The results support a mechanism wherein cyclization of the substrate Cys results in cleavage of the Cys-tRNA ester bond. Protein side chains do not play a significant role in YbaK catalysis. Instead, protein backbone atoms play crucial roles in stabilizing the transition state, while the product is stabilized by the 2'-OH of the tRNA.

Keywords

YbaK; aminoacyl-tRNA; post-transfer editing mechanism; β-thiolactone; QM/MM

Introduction

Aminoacyl-tRNA synthetases (aaRSs) play a fundamental role in establishing faithful translation through a two-step aminoacylation reaction that establishes the genetic code linkage between an amino acid and its cognate tRNA anticodon.[1] AaRS-catalyzed aminoacylation occurs via a universally conserved two-step reaction: (i) activation of amino acid with ATP to form an aminoacyl-adenylate intermediate, and (ii) transfer of the activated amino acid to form aminoacyl-tRNA. Owing to the similarity of many amino acids, some aaRSs are unable to effectively discriminate between cognate and noncognate amino acids, and have therefore developed proofreading mechanisms.[2] Error correction may occur either before ("pre-transfer") or after ("post-transfer") the activated amino acid is

[*]Address: Karin Musier-Forsyth, Department of Chemistry and Biochemistry, The Ohio State University, 100 West 18th Ave, Columbus, OH 43210, Phone: 614-292-2021. Fax: 614-688-5402. musier@chemistry.ohio-state.edu.
[⊥]Present address: B-9, Bioscience Division, Los Alamos National Laboratory, Los Alamos, NM 87545, USA

ASSOCIATED CONTENT

Supporting Information Available. Structure of QM atoms used in hybrid QM/MM calculations and energetics of *E. coli* YbaK mechanism and geometries of the β-thiolactone product formation. Additional biochemical data for YbaK mutants. This material is available free of charge via the Internet at http://pubs.acs.org.

transferred to the tRNA.[3] Editing of mischarged aminoacyl-tRNAs may be carried out by *cis*-editing domains appended to the core of the aaRS, or by free-standing editing domains that function *in trans*.[4–7] The absence of these editing mechanisms results in statistical mutations in the proteome.[8]

The inherent ability of smaller or isosteric amino acids to bind in a pocket designed for the cognate substrate poses a fundamental problem to the aminoacylation reaction. A "double-sieve" mechanism of post-transfer editing is one solution used by some aaRSs.[9] The aminoacylation active site serves as the first or "coarse" sieve, and its role is to exclude amino acids larger than the cognate substrate. The second "fine" sieve selectively binds mis-acylated amino acids and hydrolyzes them while excluding the cognate amino acid. Thus, the second sieve, which is a separate active site distinct from the synthetic active site, acts as a checkpoint to enhance fidelity.

Most bacterial prolyl-tRNA synthetases (ProRS) contain an editing domain (INS) responsible for Ala-specific editing activity.[10–12] However, ProRSs from all three kingdoms of life not only misactivate noncognate Ala but also misactivate chemically distinct Cys.[10,13] Surprisingly, ProRSs lack a Cys-specific editing activity.[13] Whereas the smaller Ala residue is bound and hydrolyzed by the INS domain, the editing domain rejects Cys, which is very similar to Pro in molecular volume. Thus a double-sieve mechanism is sufficient to clear mischarged Ala-tRNA^{Pro}, whereas a distinct post-transfer editing mechanism that does not rely on steric exclusion is needed to edit mis-acylated Cys-tRNA^{Pro}. Indeed, the latter is hydrolyzed by the single-domain YbaK protein,[5,14] which shares significant sequence and structural homology with the INS domain of bacterial ProRS. Thus, a "triple-sieve" mechanism of editing is used to hydrolyze Cys-tRNA^{Pro}, with YbaK functioning as the third sieve *in trans*.[5,15]

YbaK and INS are members of a larger "YbaK superfamily" that is widely distributed among all three kingdoms. The six members of the YbaK superfamily (ProRS INS, YbaK, PrdX, ProX, YeaK and PA2301) share significant sequence and structural homology.[16–18] Collectively, extensive biochemical and computational studies support a mechanism of YbaK catalysis that exploits the special side chain chemistry of Cys.[19] In contrast, the INS domain employs a size-exclusion based mechanism to accept and hydrolyze mischarged Ala-tRNA^{Pro}.[20]. A detailed investigation revealed that the editing reaction occurs via general water-mediated hydrolysis using both substrate and INS backbone functional groups.[21]

Here, we continue to probe the detailed mechanism of Cys-deacylation by *Escherichia coli* YbaK using a combination of biochemical assays and hybrid quantum mechanical/molecular mechanics (QM/MM) methods. We considered the roles of putative active site residues, as well as substrate functional groups in substrate specificity and catalysis. Taken together with previous work, these studies reveal both similarities and differences between the mechanism of catalysis employed by the INS domain of ProRS and the homologous YbaK protein.

Methods

Materials

All amino acids and standard chemicals were purchased from Sigma unless otherwise noted. [^{14}C]Alanine (160 Ci/mmol) and [^{35}S]cysteine (1075 Ci/mmol) were from PerkinElmer. 2'-Fluoro-2'-deoxyadenosine-5'-triphosphate (2'-F-dATP) and 2'-amino-2'-deoxyadenosine-5'-triphosphate (2'-NH_2-dATP) were from Trilink Biotechnologies.

Protein expression and purification

Histidine-tagged wild-type (WT) *E. coli* ProRS,[12] WT *E. coli* alanyl-tRNA synthetase (AlaRS),[22] WT *E. coli* cysteinylnyl-tRNA synthetase (CysRS)[23] and WT *E. coli* tRNA nucleotidyl transferase (NTase)[24] were purified using the His-select nickel affinity gel (Sigma) as previously described. The substitution mutants of *E. coli* YbaK were generated from plasmid (pET15b-*ybaK*) encoding WT *E. coli* YbaK protein using the QuikChange site-directed mutagenesis kit (Stratagene). Mutations were confirmed by DNA sequencing (Genewiz). WT and all *E. coli* YbaK variants were overexpressed in BL21(DE3) cells and purified as described for WT *E. coli* ProRS. The concentrations of *E. coli* YbaK, AlaRS, CysRS and NTase enzymes were determined by the Bradford assay[25] while the concentration of *E. coli* ProRS was determined by active site titration.[26]

Preparation of tRNAs

WT *E. coli* $tRNA^{Pro}$ and the G1:C72,U70 variant,[27] as well as WT *E. coli* $tRNA^{Cys}$ were prepared by *in vitro* transcription as described.[28,29] To prepare 3'-end modified $tRNA^{Cys}$, the 3'-terminal adenosine was exchanged with ATP analogs (2'-deoxy-, 2'-fluoro-, or 2'-amino-dATP) by incubating 45 μM $tRNA^{Cys}$ with 15 μM *E. coli* NTase and 5 mM analog in 20 mM glycine/NaOH (pH 9.0), 20 mM $MgCl_2$ and 1 mM sodium pyrophosphate. Reactions were incubated for 4 h at 37 °C and residual WT $tRNA^{Cys}$ was inactivated by oxidation with $NaIO_4$ as described.[30]

Preparation of aminoacyl-tRNA substrates

G1:C72,U70 [^{14}C]-Ala-$tRNA^{Pro}$ was prepared by incubating the tRNA (8 μM) with 4 μM WT *E. coli* AlaRS and [^{14}C]-Ala (330 μM) in 50 mM HEPES (pH 7.5), 4 mM ATP, 20 mM KCl, 20 mM β-mercaptoethanol, 25 mM $MgCl_2$, and 0.1 mg/ml bovine serum albumin for 4 h at 25 °C. WT [^{35}S]-Cys-$tRNA^{Pro}$ and [^{35}S]-Cys-$tRNA^{Cys}$ variants (WT and 3'-end modified) were prepared by incubating the tRNAs (10 μM) with 8 μM *E. coli* ProRS or 2 μM *E. coli* CysRS, respectively, [^{35}S]-Cys (0.9 μM) and unlabeled Cys (50 μM) in 20 mM Tris-HCl (pH 7.5), 20 mM KCl, 10 mM $MgCl_2$, 25 mM dithiothreitol and 2 mM ATP for 1 h at 37 °C.[19] Following aminoacylation, aminoacyl-tRNAs were phenol-chloroform extracted, ethanol precipitated, resuspended in diethylpyrocarbonate-treated water and stored at −80 °C for use in deacylation assays.

Deacylation assays

Deacylation of G1:C72,U70 [^{14}C]Ala-$tRNA^{Pro}$, WT [^{35}S]-Cys-$tRNA^{Pro}$ and [^{35}S]-Cys-$tRNA^{Cys}$ (WT and 3'-end-modified) was carried out according to published protocols.[15,19] Reactions were performed using ~0.5–1 μM aminoacyl-tRNAs and 0.5–3 μM WT *E. coli* or mutant YbaK in buffer containing 150 mM KPO_4 (pH 7.0), 5 mM $MgCl_2$, and 0.1 mg/ml bovine serum albumin. A background reaction lacking enzyme was also performed in each case. The reactions were monitored by precipitating the tRNA on Whatman 3MM filter pads followed by scintillation counting.[5] The fraction of aminoacyl-tRNA remaining was plotted as a function of time following subtraction of the buffer-only background reaction, and fitted to a single-exponential equation to obtain k_{obs}. All assays were carried out in triplicate.

Computational methods

The structural model of *E. coli* YbaK bound to the Cys-$tRNA^{Pro}$ analog 5'-CCA-Cys was generated by homology modeling using the previously reported model of *Haemophilus influenzae* YbaK bound to this substrate.[19] The structure was charge-neutralized by addition of Cl^- counterions, solvated in an 8 Å octahedral shell of TIP3P[31] waters and optimized using the ff03[32] force field in AMBER10.[33] The structure was further optimized using the hybrid QM/MM method as described below.

Hybrid QM/MM calculations

All QM/MM optimizations were carried out using ChemShell[34,35] as an interface to TURBOMOLE (v5.10)[36] for the QM atoms, and ChemShell's internal version of DL_POLY[37] for the MM treatment using the CHARMM force field.[38] Geometry optimization was carried out using the DL-FIND optimizer, employing the Broyden–Fletcher–Goldfarb–Shanno (BFGS) method. The QM layer was treated using density functional theory (DFT) with RI approximation,[39] specifically the BP86[40,41] functional with the SV(P)[42] basis set, and single-point energy calculations were carried out for each optimized geometry with the same functional and the TZVPP[43] basis set (hence, BP86/TZVPP//BP86/SV(P)). A total of 128 atoms were included in the QM layer and consisted of the ribose moiety of terminal A76, the phosphate of C75, the substrate Cys, side chains of Asn28, Ser129, and Asp136 residues, backbone atoms of Asn28-Gly30 and Leu99-Ser104 residues, and three structural waters (Supplementary Figure 1). All residues with any atom within 8 Å of the substrate Cys were optimized with MM treatment, while the remaining residues were frozen. The QM and MM regions were coupled via electrostatic embedding, with electrostatic interactions handled by the QM code with QM polarization. Potential energy surface scans were carried out by varying the reaction coordinate, defined as the difference between the Cys-C(O)–O3'-A76 (bond cleaved) and Cys-C(O)–S-Cys (bond formed), and optimizing all other degrees of freedom at each step of the fixed reaction coordinate.

Results and Discussion

Changing the size of the active site pocket does not modulate YbaK substrate specificity

YbaK residue Gly30 aligns with conserved Ile263 in the homologous ProRS INS editing domain based on structural alignment of the two domains (Supplementary Figure 2) and is highly conserved either as glycine or alanine throughout the YbaK subfamily (Supplementary Figure 3). Mutation of Ile263 to the smaller Ala residue has been shown to switch the substrate specificity of ProRS from Ala-tRNA^{Pro} to Cys-tRNA^{Pro}. To determine if the converse is true, we substituted Gly30 of *E. coli* YbaK with larger residues, such as Ile, Val or Cys, and tested the ability of these variants to hydrolyze Cys-tRNA^{Pro} and Ala-tRNA^{Pro}. All variants showed significantly reduced (>100–fold) Cys-tRNA^{Pro} deacylation activity compared to the WT enzyme (Figure 1A) and failed to gain Ala-tRNA^{Pro} deacylation activity (Figure 1B). When higher enzyme concentrations were used (3 μM), low rates of Cys-tRNA^{Pro} deacylation could be measured (Supplementary Figure 4), suggesting that substitution of the small Gly residue with the larger side chains may impact substrate binding. Nevertheless, decreasing the size of the active site pocket via G30I/V/C substitution does not alter YbaK's substrate specificity. Taken together, these results are consistent with the hypothesis that the editing domains of ProRS and YbaK have evolved distinct mechanisms of post-transfer editing. Whereas INS uses a size-exclusion based mechanism and catalyzes Ala-tRNA^{Pro} hydrolysis via nucleophilic attack by a catalytic water molecule,[21] the YbaK mechanism involves exclusion of catalytic water from the active site and substrate-mediated catalysis.[19] Thus changing the size of the active site pocket does not modulate substrate specificity of YbaK.

Computational model of *E. coli* YbaK bound to 5'-CCA-Cys

We previously reported a model of *H. influenzae* YbaK that details the mode of substrate binding and proposed a substrate-assisted mechanism of catalysis that relies on intramolecular cyclization of the substrate Cys and elimination via a β-thiolactone intermediate.[19] The computed model and catalytic mechanism are supported by extensive mutagenesis studies, as well as analyses of the reaction products by mass spectrometry. One drawback of the earlier *H. influenzae* YbaK model is that in the available crystal structure

used for modeling, the Asn25-Phe29 loop was disordered (PDB: 1DBX). Our recent biochemical and *in silico* investigation of the mechanism of INS editing showed that this loop plays a critical role in substrate binding and catalysis.[21] Thus, using the recent crystal structure of *E. coli* YbaK (PDB: 2DXA), where the corresponding loop (Ala25-Phe29) is fully resolved, we generated a new model of *E. coli* YbaK bound to the Cys-tRNA^{Pro} substrate analog 5'-CCA-Cys. This was accomplished by homology modeling and structural optimization using hybrid QM/MM methods.

The computed model of *E. coli* YbaK shows high similarity to the *H. influenzae* YbaK model, as expected. However, there are several subtle differences in the enzyme active site, which may be critical for the catalytic mechanism (Figure 2). Similar to the previous model, the substrate is bound in a deep active-site cleft, the substrate-binding loop (residues Asp23-Gly30) lies on top of the aminoacyl substrate and prevents solvent penetration into the active site, and the Ser129 residue makes a H-bond to the amine group of the substrate (Figure 2A,B). Key differences from the previous model involve the other H-bonding interactions of the substrate amine and the orientations of the substrate carbonyl and sulfhydryl groups. The substrate amine H-bonds to the Asp136 residue, which in turn is H-bonded to Tyr20 (Figure 2B). This interaction pushes the substrate closer to the Gly30 residue relative to the previous model and allows for direct interaction of the substrate sulfhydryl group with the backbone carbonyl of Phe29 (Figure 2C). Consistent with this observation, D136A mutation results in 6-fold loss in Cys-deacylation activity of YbaK (Figure 1A). Interestingly, D136C mutation has a slightly smaller effect on YbaK activity (~ 4-fold loss in k_{obs} relative to WT), suggesting that the size of this residue is important for catalysis. The substrate carbonyl points toward the GXXXP loop, which may contribute to stabilization of the tetrahedral oxyanionic intermediate formed during the cleavage reaction. We have previously proposed a catalytic mechanism for the INS domain, wherein the backbone carbonyl of Gly261 is involved in proton transfer from the nucleophilic water to the O3' of the tRNA. In the new model of YbaK, the Phe29 carbonyl lies close to both the substrate sulfhydryl group and the O3' of the tRNA, and can be envisioned to play a similar role in proton transfer.

QM/MM investigation of the mechanism of YbaK catalysis

To evaluate the theoretical feasibility of the proposed mechanism of Cys-tRNA^{Pro} cleavage by YbaK via Cys cyclization,[19] and to identify the microscopic steps of this process, hybrid QM/MM calculations were carried out at the BP86/TZVPP//BP86/SV(P) level of theory. The catalytic center, including the substrate and the nearby protein moieties, was treated with an *ab initio* QM approach, whereas the remainder of the protein-substrate complex was treated with empirical MM methods. The lowest energy structures at incremental values of the reaction coordinate were calculated. The reaction coordinate is defined as the difference in the bond lengths of the bond being formed (i.e., the bond between the Cys sulfur and the carbonyl carbon) and the bond to be cleaved (i.e., the ester bond between Cys and the tRNA). During the QM/MM calculations, only the reaction coordinate was constrained, while all other degrees of freedom were optimized. For the reactant and the product geometries, no constraints were applied.

The potential energy surface of the YbaK-catalyzed reaction shows a two-step mechanism. The lowest energy structures of the reactant, transition states, intermediate and the product are shown in Figure 3. Potential energies and the change in bond lengths of the bond being formed and cleaved are shown in Figure 4 A, B. The effect of basis set choice on the energy calculations is summarized in Supplementary Table 1. In the first step, the bond between the substrate sulfur and the carbonyl carbon is formed (Supplementary Figure 5), leading to the formation of a tetrahedral oxyanionic intermediate. This step is facilitated by the transfer of the substrate sulfhydryl proton to the backbone carbonyl atom of the Phe29 residue (Figure 4C). Protonation of the Phe29 carbonyl is stabilized by the polarization of the amide linkage

between Phe29 and Gly30 residues, where the Phe29 carbonyl is elongated and the amide bond between them is shortened (Figure 4D). The negatively charged oxygen atom of the elongated substrate carbonyl (Figure 4D) is stabilized by the oxyanionic hole formed by the GXXXP loop of the protein. The energy barrier for this step is 12.4 kcal/mol. Bond lengths associated with the formation of the β-thiolactone intermediate are shown in Supplementary Table 2.

In the second step of the reaction, the bond between Cys and the tRNA is cleaved. This step has a lower energy barrier of 3.3 kcal/mol. This step is facilitated by the transfer of a proton from the Phe29 carbonyl to the O3' of the tRNA (Figure 4C). The transition state resembles a Zundel-like complex.[44] Product formation is stabilized by the 2'-OH of the substrate, which makes a H-bond with the O3' of the tRNA and thus helps in delocalizing the electron density on this atom. The reaction product is further stabilized by the formation of a low barrier H-bond[45,46] between the nascent 3'-OH of the tRNA and the Phe29 carbonyl. The potential energy surface scan shows that the product is ~ 2 kcal/mol higher in energy than the reactant. However, since our calculations do not account for entropic contributions, it is likely that the cleaved product will have higher entropy and thus the product formation would be thermodynamically more favorable.

The products of this reaction are a four-membered β-thiolactone and the cleaved tRNA. It has been shown that β-thiolactones are highly prone to ring-opening by simple nucleophiles and can be readily hydrolyzed to yield free Cys. Because of the exclusion of water molecules from the YbaK active site, as predicted from our model, it is very likely that the β-thiolactone product is not hydrolyzed within the YbaK active site but is released and then hydrolyzed. This is consistent with previous mass spectrometric analyses of YbaK reaction products, which revealed the formation of cysteinyl-methyl ester upon reaction with solvent methanol.[19]

Role of substrate in catalysis

As for INS-catalyzed hydrolysis of Ala-tRNA^{Pro}, the mechanism of YbaK-catalyzed Cys-tRNA^{Pro} cleavage is remarkable in terms of the role played by the enzyme versus the substrate. Whereas the backbone atoms of the GXXXP loop, which stabilize the oxyanionic intermediate, and the backbone atoms of Phe29, which participate in proton transfer, contribute to catalysis, side chains of important conserved or semi-conserved residues in *E. coli* YbaK, including Tyr20, Phe29, Lys46, and Ser129, and non-conserved residue Asp136, are largely involved in substrate binding and do not appear to play active roles in catalysis.[19] On the other hand, the substrate plays a much more active role in catalysis. The sulfhydryl side chain of the Cys substrate acts as a nucleophile during catalysis, and with the exception of selenocysteine, all side chain substitutions lead to a complete loss in catalysis by YbaK.[19] Another substrate functional group, the 2'-OH of A76 of the tRNA, plays an important role in substrate binding, as well as catalysis. The 2'-OH makes a H-bond with the Gly101 amide group (Figure 2C), thus contributing to substrate binding. It also contributes to catalysis by stabilizing product formation via H-bonding to the 3'-OH of the cleaved tRNA. In support of this mechanism, we have shown that a Cys-2'-dA76-tRNA substrate analog is not cleaved by YbaK, although it acts as a competitive inhibitor of Cys-tRNA deacylation by YbaK.[19]

To further evaluate the role of the substrate 2'-OH as both a H-bond acceptor in its interaction with Gly101 and as a H-bond donor in its interaction with the 3'-O of A76, we tested additional 2'-substituted analogs of tRNA. Since 2'-deoxy-A76 tRNA^{Pro} is a poor substrate for ProRS aminoacylation,[29] tRNA^{Cys} variants were used in this study. The resulting Cys-2'-F-dA76-tRNA^{Cys} and Cys-2'-NH_2-dA76-tRNA^{Cys} variants were not substrates for YbaK catalysis (Figure 1C). The 2'-F analog retains the ability to act as a H-bond acceptor but would not serve as a H-bond donor.[47] The lack of activity with this

variant supports the proposed interaction with the 3'-O of A76. In contrast, the 2'-NH_2 analog has the ability to act as either a H-bond donor or acceptor. The lack of activity with this variant suggests that catalysis is sensitive to subtle structural changes (e.g., changes in the sugar pucker) that may result from 2' functional group substitution. Taken together, these results support a critical role for the 2'-OH group of the tRNA in substrate binding and catalysis.

Similarities and differences between YbaK and ProRS INS domain

YbaK and INS employ distinct mechanisms to maintain high selectivity for Cys-$tRNA^{Pro}$ and Ala-$tRNA^{Pro}$, respectively.[19,21] While YbaK exploits the unique chemistry of its substrate side chain, INS relies on a size-exclusion based mechanism. Despite their distinct substrate specificities and mechanisms, the two domains share several catalytic features. Both use a strictly conserved Lys residue to anchor the substrate by H-bonding to the 3'-terminal phosphate of the tRNA.[5,19] Both use polar residues to H-bond to the amine groups of the aminoacyl substrates, and a conserved GXXXP loop and terminal substrate 2'-OH to stabilize reaction intermediates and products. Finally, both enzymes appear to employ protein backbone atoms for proton transfer during catalysis rather than conserved amino acid side chains.

Major differences between the two domains lie in the sizes of their active site pockets and the exclusion of water molecules from the active site of YbaK. YbaK possesses a larger substrate binding loop (Figure 2B, 12 residues) compared to the INS domain loop (6–8 residues long). We hypothesize that the longer loop in YbaK results in the exclusion of non-structural water molecules from the active site and thus helps to maintain selectivity for Cys substrates. In contrast, the shorter substrate binding loop of INS allows water molecules to enter the active site and catalyze hydrolysis. In this case, the substrate specificity is controlled by the size of the active site pocket,[20] which can be tuned by mutagenesis to alter the substrate specificity. In contrast, the substrate specificity of YbaK could not be modulated by mutagenesis.[19]

Conclusions

The ProRS INS domain and YbaK ensure accuracy of proline codon translation by selectively clearing misacylated Ala-$tRNA^{Pro}$ and Cys-$tRNA^{Pro}$, respectively. Our previous biochemical analyses suggested that the substrate specificity of YbaK is achieved by harnessing the unique chemical properties of the substrate Cys, which can cyclize and catalyze self-cleavage.[19] As reported earlier for Ala-$tRNA^{Pro}$ hydrolysis by INS,[21] computational models of substrate-bound *H. influenzae*[19] and *E. coli* YbaK suggest that these enzymes lack conserved amino acid side chains near the ester bond to facilitate catalysis. The new experiments and *ab initio* calculations performed here support active participation of both substrate functional groups and protein backbone atoms in catalysis by YbaK (Figure 5). Taken together with previous work, our new findings shed light on the catalytic mechanisms employed by members of the YbaK superfamily of editing domains and reveal how, despite a similar overall three-dimensional protein fold, these domains have evolved to hydrolyze distinct substrates by relatively small changes in their active site architectures.

Supplementary Material

Refer to Web version on PubMed Central for supplementary material.

Acknowledgments

Generous computational resources were provided by the Ohio Supercomputer Center. Financial support for this work was provided by National Institutes of Health grant GM049928.

Abbreviations

tRNA	transfer RNA
aaRS	aminoacyl-tRNA synthetase
ProRS	prolyl-tRNA synthetase
AlaRS	alanyl-tRNA synthetase
CysRS	cysteinyl-tRNA synthetase
NTase	nucleotidyl transferase
INS	ProRS editing domain
WT	wild type
QM/MM	quantum mechanics/molecular mechanics

References

1. Ibba M, Söll D. Annu. Rev. Biochem. 2000; 69:617–650. [PubMed: 10966471]
2. Jakubowski H, Goldman E. Microbiol. Mol. Biol. Rev. 1992; 56:412–429.
3. Mascarenhas, AP.; An, S.; Rosen, AE.; Martinis, SA.; Musier-Forsyth, K. Protein Engineering. Vol. Vol. 22. Berlin Heidelberg: Springer; 2009. p. 155-203.
4. Ahel I, Korencic D, Ibba M, Söll D. Proc. Natl. Acad. Sci. USA. 2003; 100:15422–15427. [PubMed: 14663147]
5. An S, Musier-Forsyth K. J. Biol. Chem. 2004; 279:42359–42362. [PubMed: 15322138]
6. Chong YE, Yang X-L, Schimmel P. J. Biol. Chem. 2008; 283:30073–30078. [PubMed: 18723508]
7. Ling J, Reynolds N, Ibba M. Annu. Rev. Microbiol. 2009; 63:61–78. [PubMed: 19379069]
8. Li L, Boniecki MT, Jaffe JD, Imai BS, Yau PM, Luthey-Schulten ZA, Martinis SA. Proc. Natl. Acad. Sci. USA. 2011
9. Fersht, AR. Enzyme Structure and Mechanism. San Francisco: Freeman; 1977.
10. Ahel I, Stathopoulos C, Ambrogelly A, Sauerwald A, Toogood H, Hartsch T, Söll D. J. Biol. Chem. 2002; 277:34743–34748. [PubMed: 12130657]
11. Wong FC, Beuning PJ, Silvers C, Musier-Forsyth K. J. Biol. Chem. 2003; 278:52857–52864. [PubMed: 14530268]
12. Wong F-C, Beuning PJ, Nagan M, Shiba K, Musier-Forsyth K. Biochemistry. 2002; 41:7108–7115. [PubMed: 12033945]
13. Beuning PJ, Musier-Forsyth K. J. Biol. Chem. 2001; 276:30779–30785. [PubMed: 11408489]
14. Ruan B, Söll D. J. Biol. Chem. 2005; 280:25887–25891. [PubMed: 15886196]
15. An S, Musier-Forsyth K. J. Biol. Chem. 2005; 280:34465–34472. [PubMed: 16087664]
16. Crepin T, Yaremchuk A, Tukalo M, Cusack S. Structure (London, England: 1993). 2006; 14:1511–1525.
17. Zhang H, Huang K, Li Z, Banerjei L, Fisher KE, Grishin NV, Eisenstein E, Herzberg O. Proteins: Struct. Funct. Bioinform. 2000; 40:86–97.
18. Murayama K, Kato-Murayama M, Katsura K, Uchikubo-Kamo T, Yamaguchi-Hirafuji M, Kawazoe M, Akasaka R, Hanawa-Suetsugu K, Hori-Takemoto C, Terada T, et al. Acta Crystallogr. Sect. F Struct. Biol. Cryst. Commun. 2005; 61:26–29.
19. So BR, An S, Kumar S, Das M, Turner DA, Hadad CM, Musier-Forsyth K. J. Biol. Chem. 2011; 286:31810–31820. [PubMed: 21768119]

20. Kumar S, Das M, Hadad CM, Musier-Forsyth K. J. Biol. Chem. 2012; 287:3175–3184. [PubMed: 22128149]
21. Kumar S, Das M, Hadad CM, Musier-Forsyth K. J. Phys. Chem. B. 2012; 116:6991–6999. [PubMed: 22458656]
22. Beebe K, de Pouplana LR, Schimmel P. EMBO J. 2003; 22:668–675. [PubMed: 12554667]
23. Newberry KJ, Hou Y-M, Perona JJ. EMBO J. 2002; 21:2778–2787. [PubMed: 12032090]
24. Nordin BE, Schimmel P. J. Biol. Chem. 2002; 277:20510–20517. [PubMed: 11923317]
25. Bradford MM. Anal. Biochem. 1976; 72:248–254. [PubMed: 942051]
26. Fersht AR, Ashford JS, Bruton CJ, Jakes R, Koch GLE, Hartley BS. Biochemistry. 1975; 14:1–4. [PubMed: 1109585]
27. Liu H, Kessler J, Peterson R, Musier-Forsyth K. Biochemistry. 1995; 34:9795–9800. [PubMed: 7542924]
28. Beuning PJ, Musier-Forsyth K. Proc. Natl. Acad. Sci. USA. 2000; 97:8916–8920. [PubMed: 10922054]
29. Shitivelband S, Hou YM. J. Mol. Biol. 2005; 348:513–521. [PubMed: 15826650]
30. Minajigi A, Francklyn CS. Proc. Natl. Acad. Sci. USA. 2008; 105:17748–17753. [PubMed: 18997014]
31. Jorgensen WL, Chandrasekhar J, Madura JD, Impey RW, Klein ML. J. Chem. Phys. 1983; 79:926–935.
32. Duan Y, Wu C, Chowdhury S, Lee MC, Xiong G, Zhang W, Yang R, Cieplak P, Luo R, Lee T, et al. J. Comput. Chem. 2003; 24:1999–2012. [PubMed: 14531054]
33. Case, DA.; Darden, TA.; Cheatham, ITE.; Simmerling, CL.; Wang, J.; Duke, RE.; Luo, R.; Crowley, M.; Walker, RC.; Zhang, W., et al. AMBER 10. University of California; 2008.
34. Chemshell. A Computational Chemistry Shell. see www.chemshell.org.
35. Sherwood P, de Vries AH, Guest MF, Schreckenbach G, Catlow CRA, French SA, Sokol AA, Bromley ST, Thiel W, Turner AJ, et al. J. Mol. Struct. 2003; 632:1–28.
36. TURBOMOLE V5–10 2008, a development of University of Karlsruhe and Forschungszentrum Karlsruhe GmBH, 1989–2007, TURBOMOLE GmBH, since 2007. available from http://www.turbomole.com.
37. Smith W, Forester TR. J. Mol. Graphics. 1996; 14:136–141.
38. MacKerell AD, Bashford D, Bellott, Dunbrack RL, Evanseck JD, Field MJ, Fischer S, Gao J, Guo H, Ha S, et al. J. Phys. Chem. B. 1998; 102:3586–3616.
39. Weigend F. Phys. Chem. Chem. Phys. 2006; 8:1057–1065. [PubMed: 16633586]
40. Becke AD. Phys. Rev. A. 1988; 38:3098–3100. [PubMed: 9900728]
41. Perdew JP. Phys. Rev. B: Condens. Matter. 1986; 33:8822–8824. [PubMed: 9938299]
42. Schäfer A, Horn H, Ahlrichs R. J. Chem. Phys. 1992; 97:2571–2577.
43. Weigend F, Häser M, Patzelt H, Ahlrichs R. Chem. Phys. Lett. 1998; 294:143–152.
44. Zundel G, Metzger H. Z. Phys. Chem. 1968; 58:225–245.
45. Cleland WW, Kreevoy MM. Science. 1994; 264:1887–1890. [PubMed: 8009219]
46. Tuckerman ME, Marx D, Klein ML, Parrinello M. Science. 1997; 275:817–820. [PubMed: 9012345]
47. Forconi M, Schwans Jason P, Porecha Rishi H, Sengupta Raghuvir N, Piccirilli Joseph A, Herschlag D. Chem. Biol. 2011; 18:949–954. [PubMed: 21867910]

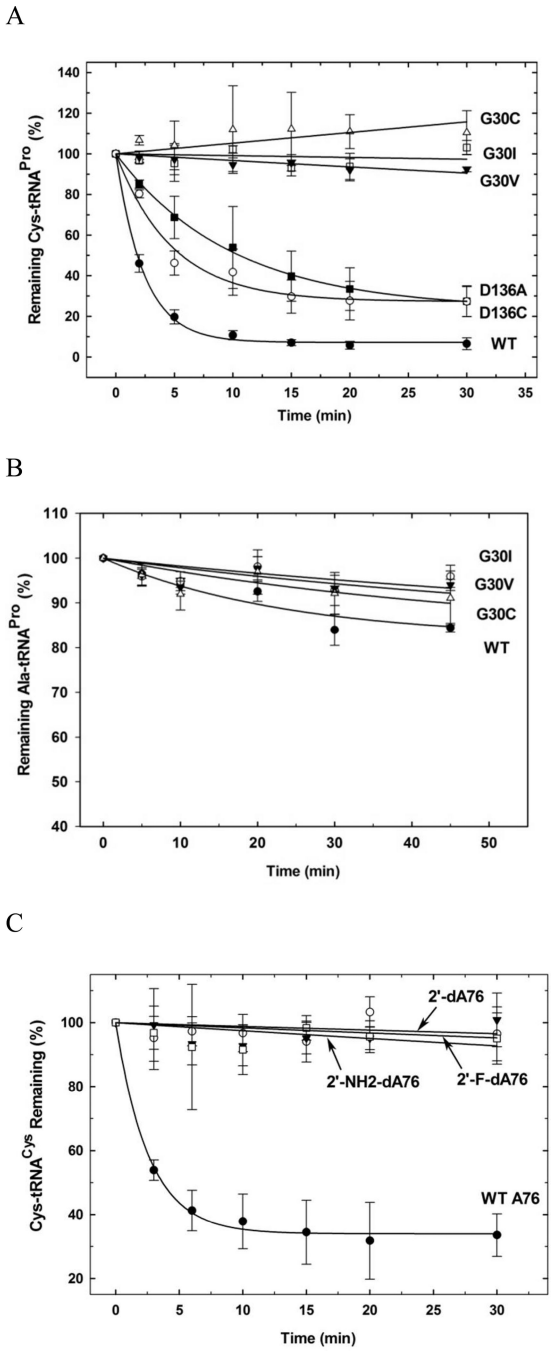

Figure 1. Effect of changes in the enzyme active site or the substrate functional groups on deacylation by *E. coli* YbaK

(A) Deacylation of 0.5 μM WT [^{35}S]Cys-tRNA^{Pro} by 0.5 μM WT YbaK (●) and YbaK variants, D136A (■), D136C (○), G30C (△), G30I (□) and G30V (▼) at 37 °C. **(B)** Deacylation of 1 μM [^{14}C]Ala-tRNA^{Pro} by 3 μM WT YbaK (●) and YbaK variants, G30C (△), G30I (○) and G30V (▼) at 25 °C. **(C)** Deacylation of 1 μM WT and 3'-end-modified [^{35}S]Cys-tRNA^{Cys} variants (WT (●), 2'-dA76(○), 2'-F-dA76 (▼) and 2'-NH_2-dA76 (□)) by 1 μM WT YbaK at 37 °C. All assays were performed in triplicate and corrected for buffer hydrolysis.

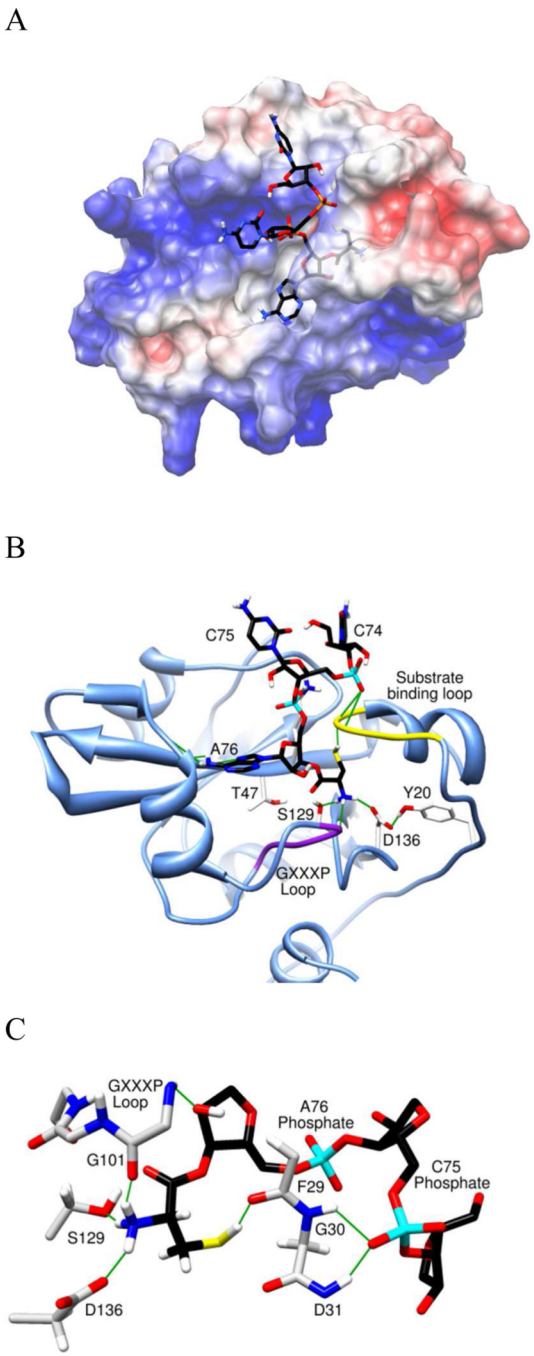

Figure 2. Computed model of *E. coli* YbaK bound to 5'-CCA-Cys substrate analog

(A) Electrostatic potential surface of the protein shows that substrate Cys is buried inside an active-site cleft. **(B)** Ribbon diagram of YbaK, showing important protein-substrate interactions. The GXXXP loop, conserved throughout the YbaK superfamily, is shown in magenta. The substrate-binding loop is highlighted in yellow. **(C)** H-bonding interactions made by the substrate Cys are shown. Substrate carbon atoms are colored black for clarity and the Cys sulfur atom is in yellow.

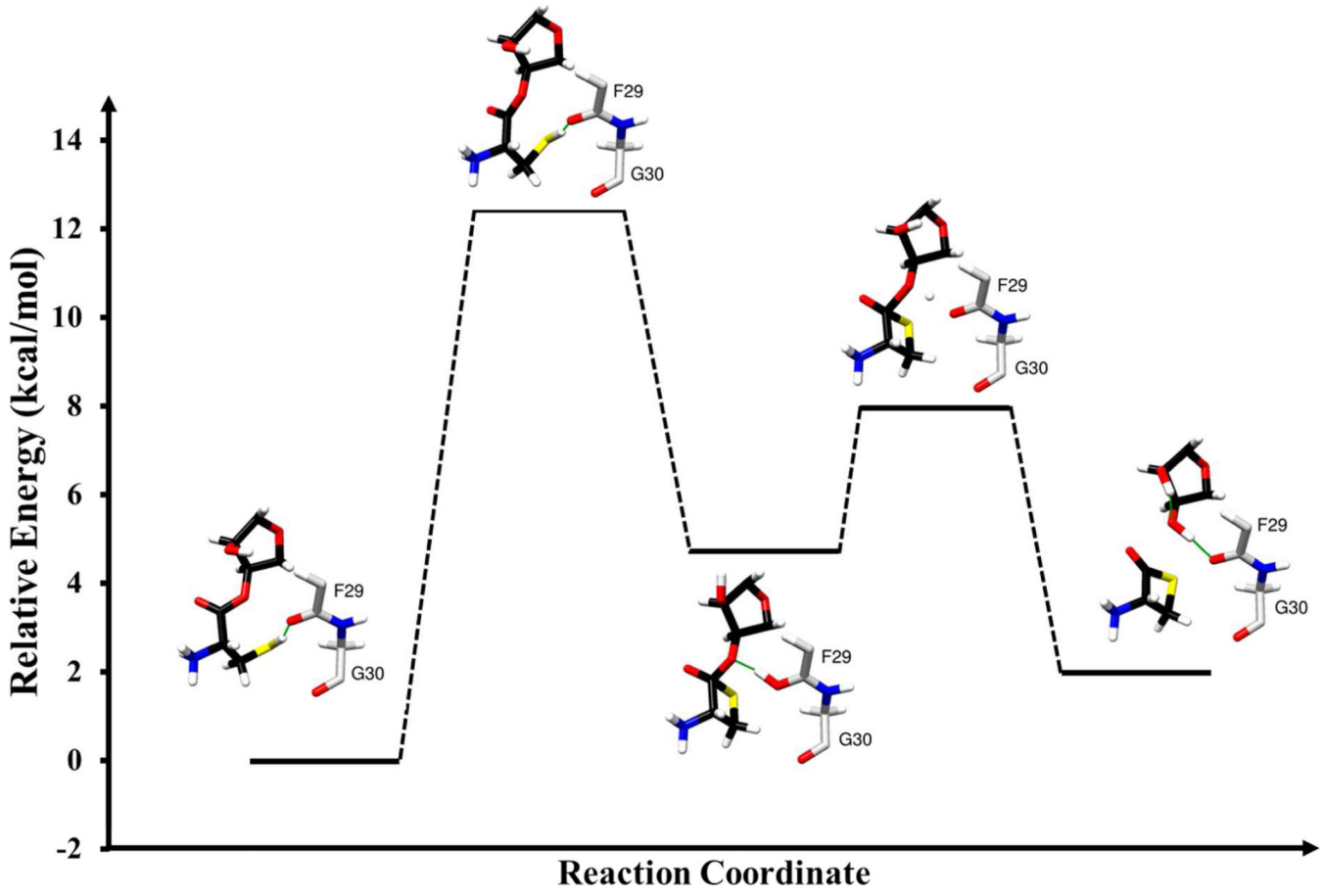

Figure 3. Potential energy surface diagram for mechanism involving cyclization of the substrate Cys by *E. coli* YbaK

The reaction coordinate is defined as the difference between the bond to be broken (Cys-C – O3'-tRNA) and bond formed (Cys-C – S-Cys). Two steps of the mechanism are depicted. In the first step, the bond between Cys-C and Cys-S is formed, leading to formation of a tetrahedral intermediate. In the second step, the bond between amino acid and the tRNA is cleaved, leading to formation of a transiently stable four-membered cyclic beta-thiolactone product.

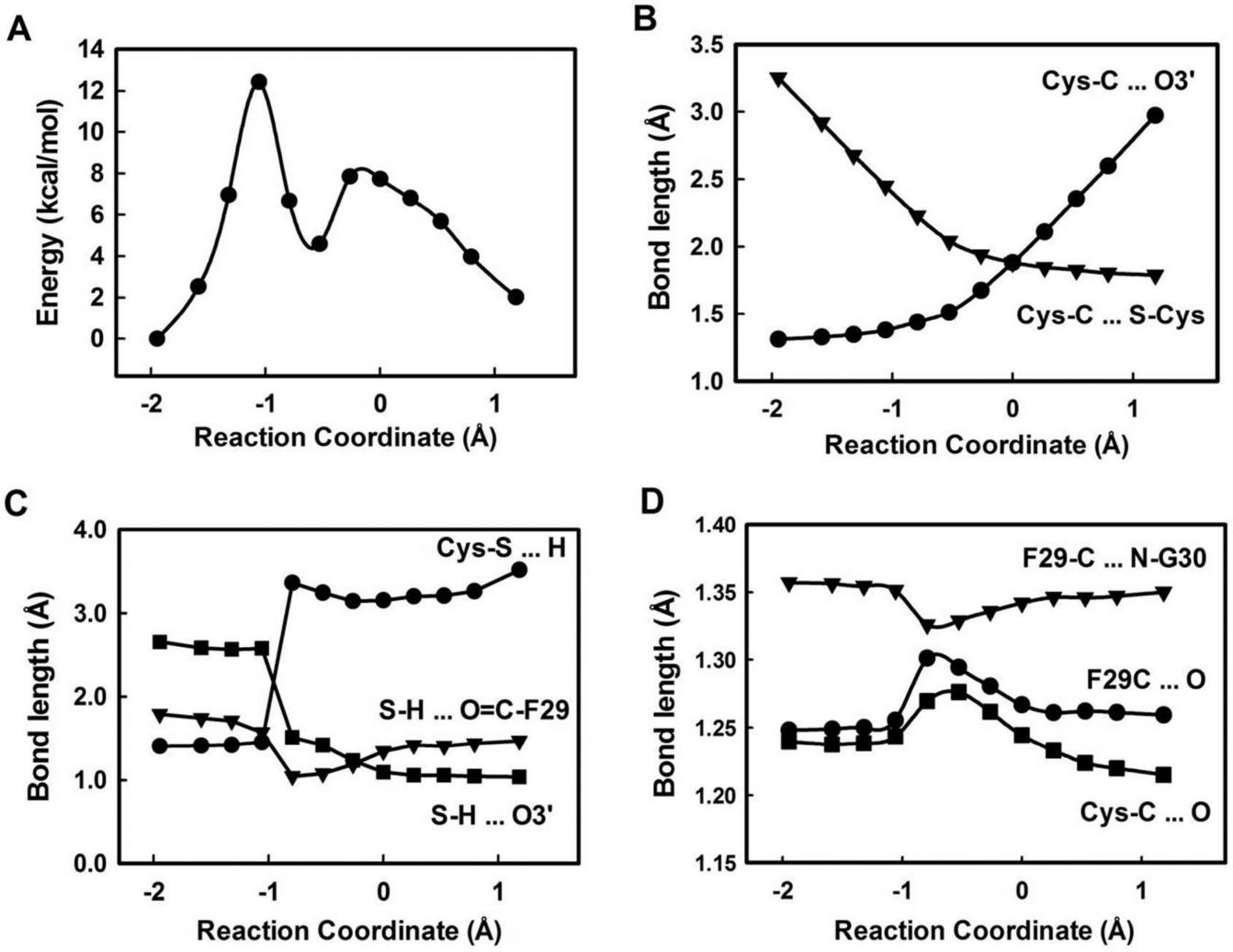

Figure 4. Energy profile and bond length perturbations during catalysis by *E. coli* YbaK

(A) Single point energy, calculated at the BP86/TZVPP//BP86/SV(P) level, as a function of the reaction coordinate. The latter is defined as the difference between the bond to be broken (Cys-C – O3'-tRNA) and the bond formed (Cys-C – S-Cys). **(B)** Bond formation between Cys-C and Cys-S (▼) and cleavage of Cys-C – O3'-tRNA bond (●) as a function of the reaction coordinate. **(C)** Mechanism of proton transfer from substrate to product. Distance of the proton being transferred from Cys-S (●), F29C=O (▼), and O3'-tRNA (■) is shown. **(D)** Change in bond lengths of substrate carbonyl (■) as a function of reaction coordinate. Elongation of this bond leads to stabilization of the tetrahedral intermediate. Proton transfer from substrate Cys to backbone carbonyl of Phe29 residue is stabilized by a polarization of the amide linkage, depicted by lengthening of the Phe29 carbonyl bond (●) and shortening of the amide linkage between Phe29 and Gly30 residues (▼).

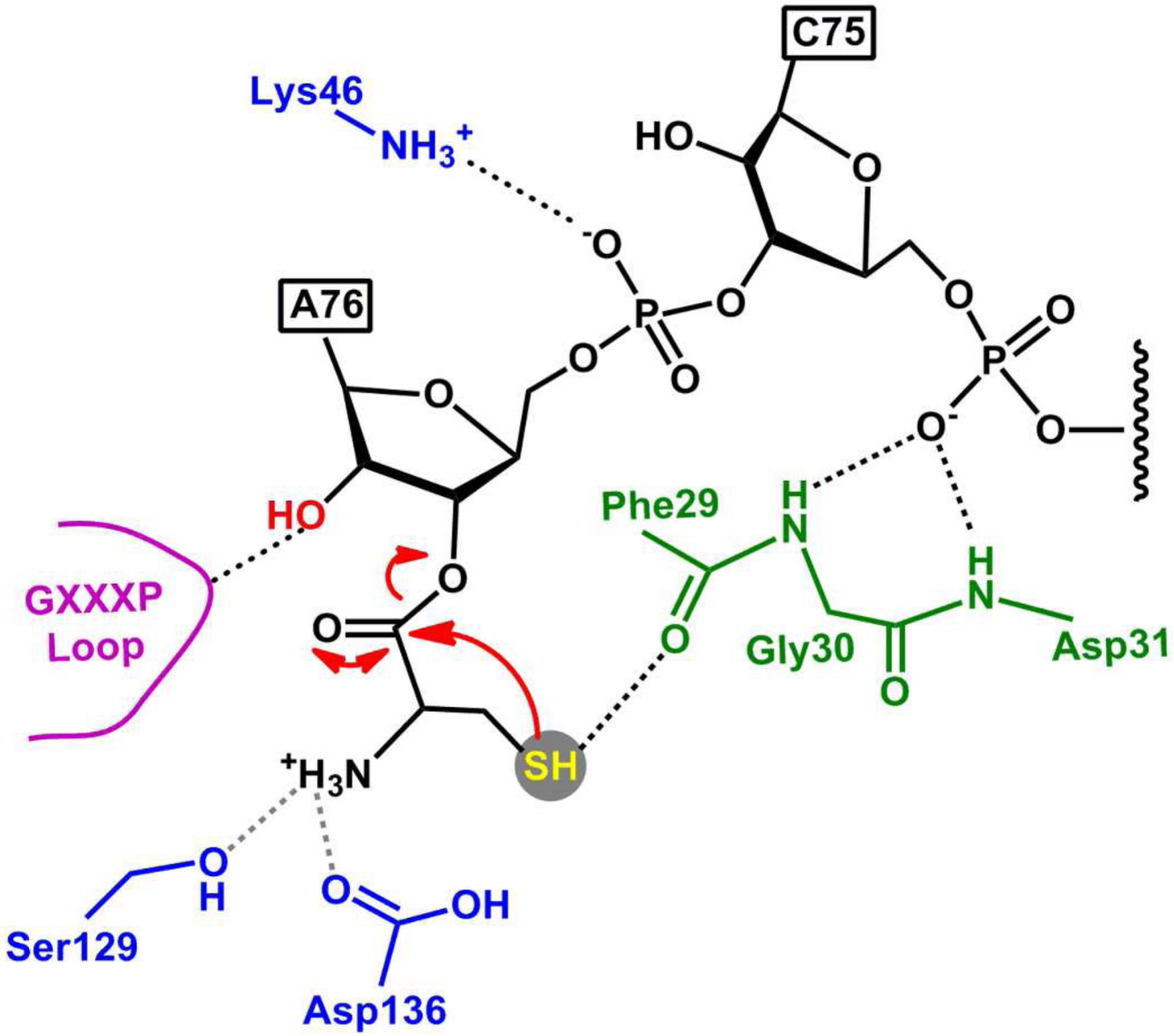

Figure 5. Model for Cys-tRNA^{Pro} deacylation by *E. coli* YbaK

Shown is a summary of proposed interactions made by the backbone and side chain residues of YbaK with the substrate Cys-tRNA in the active site pocket. The backbone carbonyl of Phe29 and amides of Phe29 and Gly30 (highlighted in green) make critical H-bonding interactions with the substrate thiol (shown in yellow) and C75 phosphate. The thiol side chain attacks the carbonyl center, leading to the cleavage of the ester bond and formation of a cyclic thiolactone intermediate. Important side chains (Lys46, Ser129 and Asp136) are shown in blue. Lys46 interacts with the A76 phosphate and stabilizes the substrate orientation in the active site pocket. Ser129 and Asp136 side chains H-bond and stabilize the substrate Cys amine. The tetrahedral oxyanionic transition state is stabilized by the GXXXP loop (magenta).